

Constrained simulations of the local universe: I. Mass and motion in the Local Volume

Luis A. Martinez-Vaquero¹, Gustavo Yepes¹ and Yehuda Hoffman²

¹*Grupo de Astrofísica, Universidad Autónoma de Madrid, Madrid E-280049, Spain*

²*Racah Institute of Physics, Hebrew University, Jerusalem 91904, Israel*

9 November 2018

ABSTRACT

It has been recently claimed that there is no correlation between the distribution of galaxies and their peculiar velocities within the Local Volume (LV), namely a sphere of $R = 7 h^{-1} \text{Mpc}$ around the Local Group (LG). It has been then stated that this implies that either locally dark matter is not distributed in the same way as luminous matter, or peculiar velocities are not due to fluctuations in mass. To test that statement a set of constrained N-body cosmological simulations, designed to reproduce the main observed large scale structure, have been analyzed. The simulations were performed within the flat- Λ , open and flat matter only CDM cosmogonies. Two unconstrained simulations of the flat- Λ and open CDM models were performed for comparison. LG-like objects have been selected so as to mimic the real LG environment. The local gravitational field due to all halos found within each LV is compared with the exact gravitational field induced by all matter in the simulation. We conclude that there is no correlation between the exact and the local gravitational field obtained by pairwise newtonian forces between halos. Moreover, the local gravitational field is uncorrelated with the peculiar velocities of halos. The exact gravitational field has a linear correlation with peculiar velocities but the proportionality constant relating the velocity with gravitational field falls below the prediction of the linear theory. Upon considering all matter inside the LVs, the exact and local gravitational accelerations show a much better correlation, but with a considerable scatter independent on the cosmological models. The main conclusion is that the lack of correlation between the local gravitation and the peculiar velocity fields around LG-like objects is naturally expected in the CDM cosmologies.

Key words: methods: numerical – galaxies: Local Group – cosmology: dark matter

1 INTRODUCTION

A key ingredient of the standard model of cosmology is that the large scale structure (LSS) has emerged out of an otherwise a homogenous and isotropic universe *via* gravitational instability (e.g. Peebles (1980)). One of the main consequences of gravitational instability is that the growth of structure induces a non-vanishing velocity field. The standard model of cosmology relates the large scale mass density and peculiar velocity fields. It further assumes that the observed galaxy distribution is closely related with the underlying matter density field, even if this relation is biased in some yet unknown way. In an interesting recent paper Whiting (2005) (W05) has challenged these basic ideas of the standard model by testing them against a study of the galaxy distribution and their peculiar velocities in the Local Volume (LV), defined as the sphere of radius

$R = 7 h^{-1} \text{Mpc}$ (where h is the Hubble’s constant in units of $100 \text{ km s}^{-1} \text{Mpc}^{-1}$) centred on the Local Group (LG). W05’s main conclusion is that *‘Either dark matter is not distributed in the same way as luminous matter in this region, or peculiar velocities are not due to fluctuations in mass.’* This is a very important result and if it was true it would put the standard model of cosmology on very shaky foundations. The main goal of our paper is to examine W05 methodology and claims by analyzing the kinematics and dynamics of simulated LV systems in different cosmological models. As we will show in this paper, our numerical results do not support W05’s claims.

W05 carried out an analysis of the distribution and peculiar velocities of 149 galaxies in the LV. Using the high-quality data of these galaxies W05 has mapped the mass distribution within the LV, assuming it is traced by the galaxies, and calculated the gravitational field within the

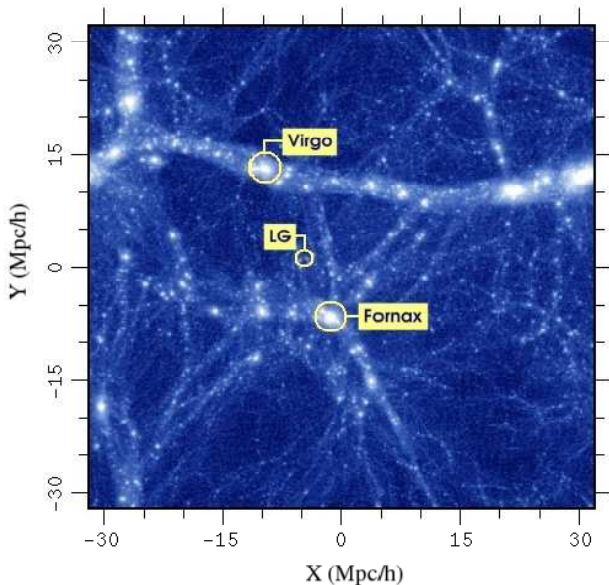


Figure 1. Projected dark matter distribution for the Λ CDM constrained simulation. The image shows a projected slice of $10 h^{-1}$ Mpc thick across the box centre in supergalactic coordinates X and Y. The Local Supercluster is the filament crossing the box horizontally. The position of the Local Group and the Virgo and Fornax clusters are shown.

LV. The gravitational field has been calculated by summing over the pairwise Newtonian interaction for each galaxy and by weighting the galaxies by their K and B luminosity. W05’s working assumption is that the peculiar velocity of galaxy should be aligned with the gravitational field it experiences and that the amplitude of the peculiar velocity and gravity fields should be linearly connected. The notion that ‘the peculiar velocity field is linear with the gravitational field’ is strictly valid in the linear regime of the gravitational instability in an expanding universe. If such a linear relation had been confirmed by the high-quality data that the LV provides this would have validated the idea that the LSS is indeed induced by gravitational instability. No clear correlation was found between the velocity and local gravitational fields. This has led W05 to conclude that, at least in the LV, structure has not formed by means of the gravitational instability.

The above conclusion should be tested carefully. The main goal of the present paper is to apply W05 analysis to a set of N-body constrained simulations (CSs) of the local universe. The CSs are designed to reproduce the gross features of the nearby universe, namely the main players of the nearby LSS, such as the Local Supercluster (LSC) and the Virgo, are imprinted onto the simulations (Kravtsov et al. 2002; Mathis et al. 2002; Klypin et al. 2004; Dolag et al. 2005; Hoffman et al. 2006). This is achieved by setting the initial conditions of the simulations as constrained realizations of Gaussian fields, where actual observational data is used as constraints. The CSs provide an almost optimal laboratory for testing W05 algorithm, as they closely mimic the dynamics of the LV. CSs have been run in the framework of the benchmark flat- Λ CDM model as well as in the open CDM (OCDM) and the so-called flat matter only standard

Model	Ω_m	Ω_Λ	h	σ_8
Λ CDM	0.3	0.7	0.7	0.9
OCDM	0.3	0	0.7	0.9
SCDM	1.0	0	0.5	0.7

Table 1. Cosmological parameters used for the different CDM models

CDM (SCDM) models. In addition, W05 procedure has been tested against standard, non-constrained, simulations of the same models.

This is a first in a series of papers that focuses on studying the nearby universe by means of N-body and hydrodynamical CSs. In particular issues concerning the coldness of the local flow, the mass distribution in the LV, the mass accretion history of the LG and the future of the nearby structure in a dark energy dominated universe are to be addressed. The highlight of this project will be the full galaxy formation high resolution simulation of the LG. Our choice of the different models is dictated by our plan to study the nature of the velocity field in the LV in the CDM cosmogony and in particular its dependence on the dark energy and the dark matter. In this regard the SCDM model is considered to be an extreme case and is taken for reference. Forthcoming papers in this series will focus on the problem of the coldness of the local Hubble flow.

The structure of the paper is as follows: a brief description of the simulations is given in § 2. The selection of LG-like objects is described in § 3 and the analysis itself in § 4. The results of the analyses are given in § 5. A final discussion of the results is given in § 6.

2 SIMULATIONS

W05 has analyzed one and only one particular patch of the universe, namely the LV that extends around the LG. The LG is not a unique or an unusual object in the universe, yet it has its own characteristics that affect the outcome of any dynamical test that would be applied to it. Our main goal is to check the validity of the W05 approach, in the context of the environment of the LG. This is to be achieved by applying the W05 analysis to LG-like objects found in appropriate N-body simulations. The key to a successful study is to properly select LG-like objects from the simulation and analyze the LV around these objects (see § 3). Yet the selection of the LG-like objects is based on the properties of the LG itself and not on its environment within the LV. This has encouraged us to use CSs as a ‘laboratory’ for testing the W05 procedure in conditions very similar to the ones prevail in the LV and its immediate surrounding. In addition we have used unconstrained simulations for reference. The comparison of the results obtained in the constrained and unconstrained simulations will shed light on the question of whether the findings of W05 are naturally expected in CDM dominated cosmogonies.

The data used to constrain the initial conditions of the simulations is made of two kinds. The first data set is made of radial velocities of galaxies drawn from the MARK III (Willick et al. 1997), SBF (Tonry et al. 2001) and the

Karachentsev (2005) catalogs. Peculiar velocities are less affected by non-linear effects and are used as constraints as if they were linear quantities (Zaroubi et al. 1999). This follows the CSs performed by Kravtsov et al. (2002) and Klypin et al. (2003). The other constraints are obtained from the catalog of nearby X-ray selected clusters of galaxies (Reiprich & Böhringer 2002). Given the virial parameters of a cluster and assuming the spherical top-hat model one can derive the linear overdensity of the cluster. The estimated linear overdensity is imposed on the mass scale of the cluster as a constraint. Different CSs with different random realizations have been calculated and they all exhibit a clear and unambiguous LSC-like structure that dominates the entire simulation, much in the same way as in the actual universe in which the LSC dominates the nearby LSS. The simulations do vary with respect to the particular details of the LG-like object that is formed roughly in its actual position. All simulations used here are based on the same random number realization of the initial conditions.

Five simulations have been performed so far. Three constrained ones have been performed within the framework of the Λ CDM, OCDM and SCDM models. In addition, unconstrained simulations of the Λ CDM and OCDM cosmologies have been performed for the sake of comparison and benchmarking. Table 1 presents the cosmological parameters of the different simulations. All simulations correspond to a periodic cubic box of $64 h^{-1}$ Mpc on a side. We made a random realization of the corresponding power spectrum for each cosmological model with a large number of particles (2048^3). At the same time, a constrained realization of the density field for the same power spectra was done in an Eulerian mesh of 256^3 grid points. After Fourier transforming both constrained and unconstrained density fields, we substitute the Fourier modes of the constrained field into the unconstrained one. Finally, we used Zeldovich approximation to compute the 3D displacement field for an initial redshift of $z=60$. Once we got the displacements for a refined mesh of 2048^3 grid points, we used it to estimate the initial conditions for a resampling of 256^3 dark matter particles in total. In this way, we are able to zoom into a particular area of the simulations and resimulate them with much higher resolution, up to the maximum resolution possible (2048^3), having the same structures as in the low resolution simulations (see Klypin et al. (2001) for a more detailed information about zoomed simulation techniques). Thus, all the numerical experiments that are reported here have the same number of particles (256^3). This translates into a mass per particle of $1.3 \times 10^7 h^{-1} M_\odot$ for Λ CDM and OCDM and $4.3 \times 10^7 h^{-1} M_\odot$ for SCDM simulations.

We have used the parallel TREEPM N-body code GADGET2 (Springel (2005)) to run these simulations. A uniform mesh of 512^3 grid points was used to compute the long-range gravitational force by means of the Particle-Mesh algorithm. A constant comoving Plummer equivalent gravitational smoothing scale of $20 h^{-1}$ kpc was set at high redshift and we changed it to $5 h^{-1}$ kpc physical scale since $z=3$ till $z=0$. The number of timesteps to complete the evolution from $z=60$ till $z=0$ ranges from 5000 to 7000 depending on the simulation. We employed a variety of parallel computer architectures (SGI-ALTIX, IBM-SP4, Opteron-clusters) during the course of this work. Using 16 processors simultaneously, we completed one run in about 2 cpu days.

Components	Kind	MW + M31
	Mass	$125 \leq V_c \leq 270$ km/s
	Separation	$s \leq 1$ Mpc/h
	Relative velocity	$V_r < 0$
# neighbours	Distance to LG	$d_{neigh} < 3$ Mpc/h
	Mass	$V_c \geq V_{c,comp}$
Virgo halos	Distance to LG	$5 \leq d_{Virgo} \leq 12$ Mpc/h
	Mass	$500 \leq V_c \leq 1500$ km/s

Table 2. Constrains used to find LG candidates following the Macciò *et al.* (2005) criterion. The circular velocity has been used for the mass constraints.

In what follows, we will use the name Λ CDM, OCDM and SCDM for the simulations with Constrained Initial conditions in the different cosmological models. The names Λ CDMu and OCDMu will refer to the two different unconstrained realizations in the Λ CDM and OCDM models respectively. As an example of how the simulations look like, we show in Figure 1 a projection of the dark matter distribution in the Λ CDM simulation box at $z=0$.

3 SELECTION OF LG CANDIDATES

Dark matter halos were found in simulations using two object finding methods: The Bound Density Maxima (BDM) algorithm (Klypin et al. (1999)) is based on finding local center of mass in spheres of variable radius starting from randomly selected particles in the simulation. The Amiga Halo Finder (Gill et al. (2004)), on the contrary, finds local density maxima from an adaptive mesh hierarchy. In both cases, an iterative procedure to find local centre of mass from density maxima is used. Particles that are not gravitationally bound to the halo potential are also removed. We took halos composed by more than 100 dark matter particles, which translates into a minimum mass per halo of $M_{min} = 1.3 \times 10^9 h^{-1} M_\odot$ for the Λ CDM and OCDM simulations and $M_{min} = 4.3 \times 10^9 h^{-1} M_\odot$ for the SCDM simulation. We identified the same objects with both methods. For the work reported here we have used the halo catalogues obtained by the public available AMIGA halo finder code (<http://www.aip.de/People/AKnebe/AMIGA/>).

To identify LG candidates from the halo distribution, we selected those objects that fulfill the strict requirements as given in Governato et al. (1997) and Macciò et al. (2005). They are summarized in Table 2. In brief, we searched for two halos similar to Milky Way and M31 galaxies, without neighbours with masses as high as any of the LG members and with a Virgo-like halo at an appropriate distance. A few tens of LG-like objects have been identified in each simulation (23 objects in Λ CDM, 34 in Λ CDMu, 41 in OCDM, 58 in OCDMu and 37 in SCDM). One of the LG-like object for the Λ CDM simulation which closely resembles the actual LG in terms of its mass and position, is presented in Figure 2.

4 ANALYSIS

In order to study the dynamics of the LG-like objects found in the simulations, we have first computed the local Hubble

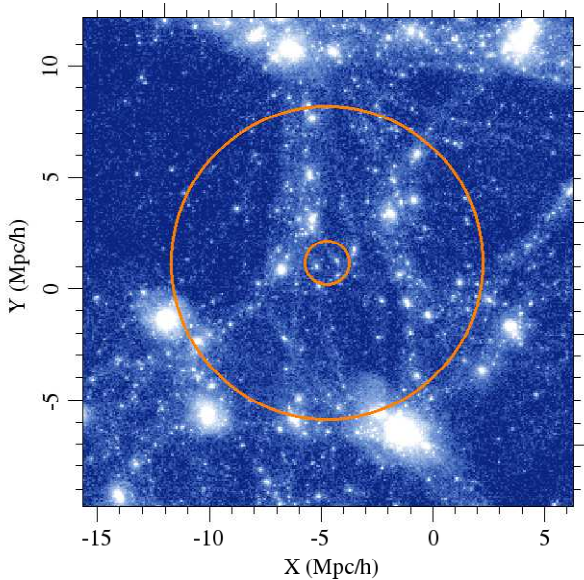


Figure 2. Projected dark matter distribution around the best LG candidate in the Λ CDM simulation in supergalactic coordinates. The outer circle delimits the Local Volume and the inner circle represents the LG position

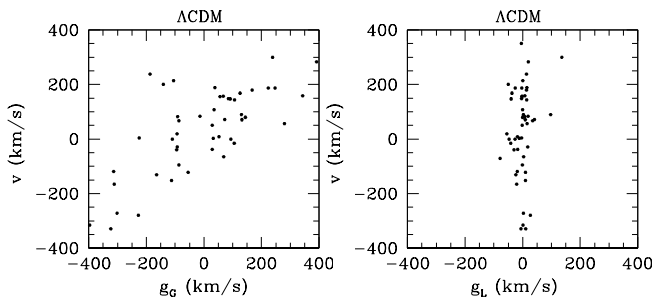


Figure 3. Plots of v vs. g_G and v vs. g_L for the candidate of Figure 2.

flow in spheres of $7 h^{-1} \text{Mpc}$ around each candidate, and have also estimated the local overdensity within these spheres from the total mass inside them. All DM halos within the LV around each LG-like objects have been identified and the gravitational field acting on each halo has been calculated in two different ways. First, the local gravitational field is calculated like in W05 by the summation over the pairwise newtonian interaction. Namely, the field acting on the i -th halo is given by

$$\tilde{\mathbf{g}}_{l,i}^{\text{tot}} = -G \sum_{j \neq i} M_j \frac{\mathbf{r}_j - \mathbf{r}_i}{[(\mathbf{r}_j - \mathbf{r}_i)^2 + A^2]^{3/2}} \cdot \hat{\mathbf{r}}_i, \quad (1)$$

where, following W05, a softening parameter of $A = 1.2 h^{-1} \text{Mpc}$ is introduced. Then we calculate also the 'true' gravitational field, namely the field calculated by the N-body code of the full mass distribution in the computational box. This is defined as the global gravitational field, (see the appendix for further information).

As in W05, the local gravitational field is decomposed into two terms, the contribution of a smooth background

of matter and a fluctuating part given by the point mass distributions. Since we are interested in deviations from the average, we have to subtract the linear term contributed by the background, \mathbf{g}_{bg} , from the local gravitation field

$$\tilde{\mathbf{g}}_i = \tilde{\mathbf{g}}_i^{\text{tot}} - \tilde{\mathbf{g}}_{bg}. \quad (2)$$

The calculation of the background term is done in two ways. First, following W05, the background solution is fitted by a linear term in \mathbf{r} . Alternatively, the background solution is calculated by the exact solution for the unperturbed universe:

$$\tilde{\mathbf{g}}_{bg} = -G \frac{4\pi}{3} \Omega_m \rho_c \mathbf{r} \quad (3)$$

The two methods give virtually identical results and the fitting method has been used here, so as to be consistent with analysis of W05. We have also subtracted the anisotropic background estimated from the tidal field (see § 5.2).

As we have mentioned earlier, the purpose of the present study is to compare gravitational accelerations and velocities. To facilitate such a comparison the gravitational field is scaled by the linear theory prediction,

$$\mathbf{g}_x = \frac{2f(\Omega_m, \Omega_\Lambda)}{3H_0\Omega_m} \tilde{\mathbf{g}}_x \quad (4)$$

where x stands here for the local or global field. The velocity-gravity scaling factor is given by

$$f(\Omega_m, \Omega_\Lambda) \approx \Omega_m^{0.6} + \frac{1}{70} \Omega_\Lambda \left(1 + \frac{1}{2} \Omega_m \right) \quad (5)$$

(e.g. Peebles (1980), Lahav et al. (1991)). Throughout the paper the gravitational fields will be represented by their scaled versions.

Our analysis is exemplified by Figure 2 which shows one of the LG-like objects in the Λ CDM constrained simulation. The figure shows the matter distribution in a box of $20 h^{-1} \text{Mpc}$ centered on the simulated LG and projected on the Supergalactic plane. In Figure 3, two scatter plots show the scatter of the local and global gravitational accelerations, v , vs. the peculiar velocity of all DM halos in this particular LV. In what follows, all quantities shown correspond to projections along the line of sight with the observer located in the center of mass of the LG candidates.

5 RESULTS

5.1 Relation between local and global accelerations

Figure 4 shows scatter plots of local vs. global gravitational fields for some of the Local Volume candidates extracted from simulations. In order to study the relation between both fields, a linear fit to the g_L vs. g_G distribution has been made for all the LG candidates found in the different simulations.

Figure 5 shows the least square fit slopes and correlation coefficients of the local to the global gravitational fields as a function of the overdensity $\delta\rho/\rho$ measured within each of the simulated LV's. We find that the local and global field are uncorrelated, showing an extremely small correlation coefficient and a mean and median slope of roughly 0.1 rather than unity.

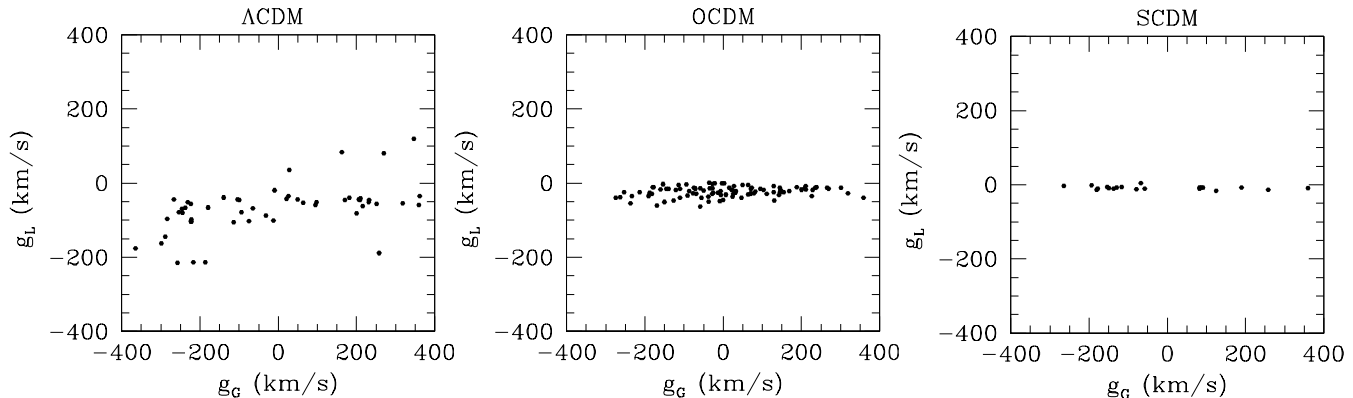


Figure 4. Local vs. global scaled acceleration for one of the LG candidates in the constrained Λ CDM, OCDM and SCDM simulations respectively.

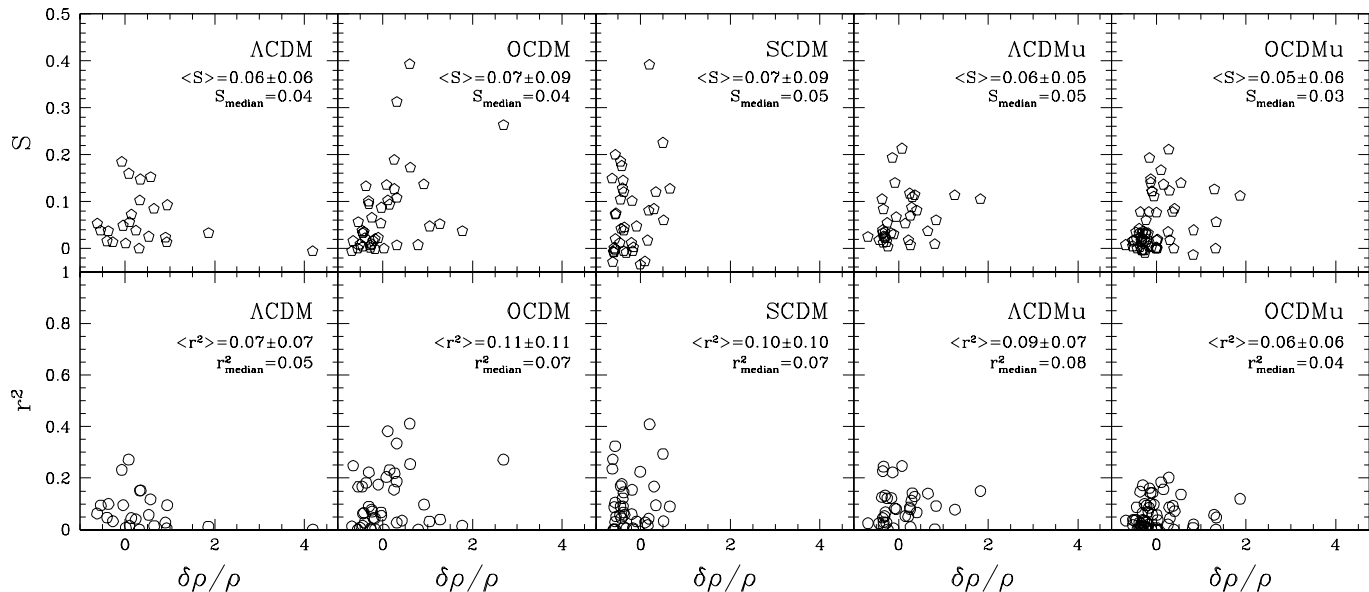


Figure 5. Slopes (first row) and Pearson's correlation coefficient (second row) of the linear fit of g_L vs. g_G as a function of overdensity calculated within the simulated Local Volumes for all candidates found in each simulation. The median and the average slope and correlation coefficient with their one sigma errors for all LGs in each simulation are also shown.

We have tested the effect of taking only haloes with high mass (more than $10^{11} h^{-1} M_{\odot}$). The results are very similar to the previous ones, because the lightest haloes do not contribute much to the gravitational field. The overdensity was calculated by computing all matter inside the local volumes. When using only mass in halos to estimate the overdensity, results do not change at all.

In the preceding analysis the local gravitational field is calculated by summing over the pairs of DM halos, assuming they carry all the mass in the LV and that their mass is spread out over a relatively large area described by the A smoothing parameter. The poor correlation between the local and global gravitational fields has led us to relax the assumption that the mass is traced by the DM halos and calculate the local field contributed by all dark matter particles in the LV. This is presented in Figure 6, which shows a very tight correlation between g_L and g_G for one particular LG-like object in the Λ CDM CS. A better correlation with a slope very close to unity are obtained when we include all

the particles that constitute the inter-halo medium, rather than by the intra-halo particles only, as can be seen in Figure 7. Moreover, the only gravitational smoothing done in this case correspond to that included in the simulation, which is of the order of kiloparsec scale, contrary to the strong smoothing of 1.2 Mpc used in W05 analysis and in our previous estimates. The horizontal branch around the origin observed in Figure 6 is mainly due to particles not bound to halos. These particles are more affected by the external field than particles bounds to halos, and therefore for these the local acceleration is much smaller than the global one.

Obviously, the correlation between the local and global acceleration improves as the LV increases. This has been checked for the LG-like object of Figure 6. Assuming a LV of a $30 h^{-1} \text{Mpc}$ radius the correlation improves to $S = 0.47$ and $r^2 = 0.58$. However this is still considerably worse than the $S = 0.89$ and $r^2 = 0.91$ obtained by considering all the particles within the $7 h^{-1} \text{Mpc}$ LV (Figure 6).

The lack of correlation between the local and global

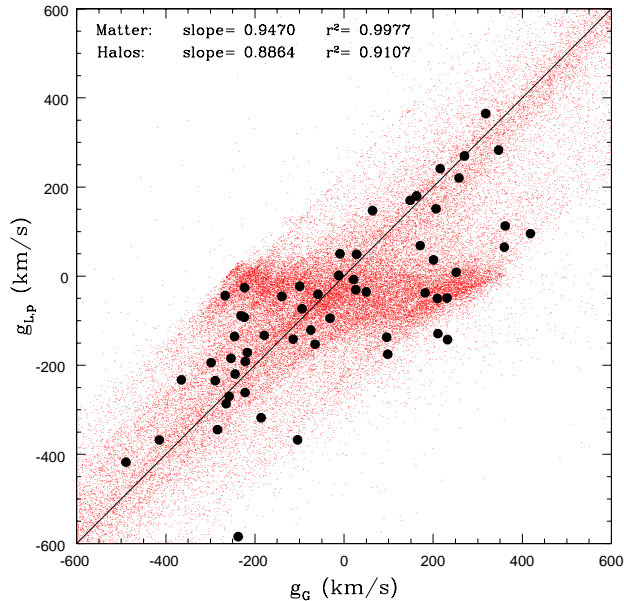


Figure 6. Local *vs.* global gravitational accelerations computed taking into account all the particles within the LV for the same candidate in the Λ CDM simulation as in Figure 4. The small points represent the individual dark matter particles. Thick solid points correspond to halos in which accelerations have been computed by the average of all particles inside them. The straight line shows the equivalence between both accelerations.

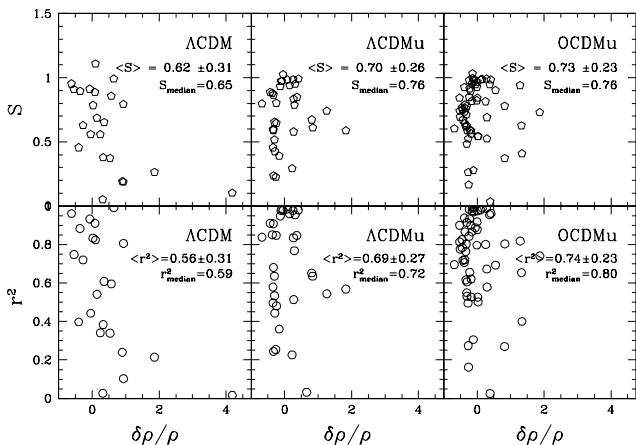


Figure 7. Slopes (first row) and Pearson's correlation coefficients (second row) for the g_L *vs.* g_G least square fits for all the LG candidates found in the Λ CDM and Ω CDM simulations as a function of overdensity. All particles within simulated LVs have been taken in the computation of the local accelerations. A gravitational smoothing parameter of $5 h^{-1}$ kpc is assumed to compute the newtonian pairwise forces between particles.

gravitational accelerations, strongly leads to expect the absence of correlation between the local gravitational field and the peculiar velocities. This is clearly confirmed by the analysis presented in § 5.2.

5.2 Accelerations and velocities

Figures 8 and 9 present the peculiar velocities as a function of the scaled global and local gravitational accelerations around some selected LG-like objects in the different simulations. The slopes and the correlation coefficients of the linear fits for the relation between the peculiar velocities and the gravitational accelerations acting on halos in the LV around all LG-like objects are given in Figures 10 and 11. The least square fit analysis confirms the visual impression of Figures 8 and 9. The peculiar velocity of halos in the LV of LG-like objects is clearly correlated with the global acceleration but with a non-negligible scatter, with a mean and median correlation coefficient around 0.5 for the constrained simulations and somewhat lower for the unconstrained ones (Figure 10). The mean and the median slope of the linear relation between the velocity and scaled global acceleration is in the range of 0.4 to 0.6. The distribution of the fitted slopes shows some dependence on the mean overdensity ($\delta\rho/\rho$) in the LV. The width of the distribution decreases with the overdensity. At low $\delta\rho/\rho$'s the slope ranges from roughly 0.2 to almost unity but at $\delta\rho/\rho \gtrsim 1$ the slope shows a narrow scatter around its mean value of ≈ 0.5 . Upon scaling of the gravitational field the linear theory predicts the slope to be unity. It follows that the amplitude of the peculiar velocities is smaller than what is expected by the linear theory.

The peculiar velocities do not show any correlation with the local accelerations (Figures 9 and 11). Their linear fit yields extremely low correlation coefficients and the fitted slope has no meaning. One should recall here that this lack of correlation has already been anticipated from the lack of correlation we found between the local and global accelerations (§ 5.1).

The calculation of the local gravitational acceleration neglects the contribution of the tidal field, which is induced by the inhomogeneous matter distribution outside of the LV. Obviously, for objects like the LG, with the Virgo cluster located just outside of the LV, the tidal field cannot be neglected. The local gravity-velocity correlation should be improved by adding the tidal field into the fitting procedure. Indeed, we follow W05 and extend the fitting procedure to

$$\sigma^2 = \frac{1}{N} \sum (g_L - v + \mathbf{v}_0 \cdot \hat{\mathbf{r}} + \hat{\mathbf{r}} \cdot \mathbf{H} \cdot \mathbf{r})^2, \quad (6)$$

where \mathbf{v}_0 is an unknown vector and \mathbf{H} is a symmetrical tensor with six unknown quantities. The nine free parameters are found by minimizing the scatter. Note that in the limit of the linear theory and for a small LV \mathbf{v}_0 should be set to zero and the symmetric tensor H should be traceless. As the above assumptions do not hold for the LG we allow for a finite \mathbf{v}_0 and for H to have a trace.

Figure 12 shows that indeed adding the \mathbf{v}_0 and \mathbf{H} terms improves somewhat the correlation between the local gravity and peculiar velocities. Yet, they are weakly correlated with $r^2 \approx (0.1 - 0.2)$ for most LG-like objects. The minor improvement is not surprising. The Virgo cluster is located at a distance of about $10 h^{-1}$ Mpc and the LV is defined by a sphere of radius of $7 h^{-1}$ Mpc. Hence, modeling the tidal field by a spatial linear expansion, as is implicitly assumed in Eq. 6 constitutes a poor fit of the tidal field.

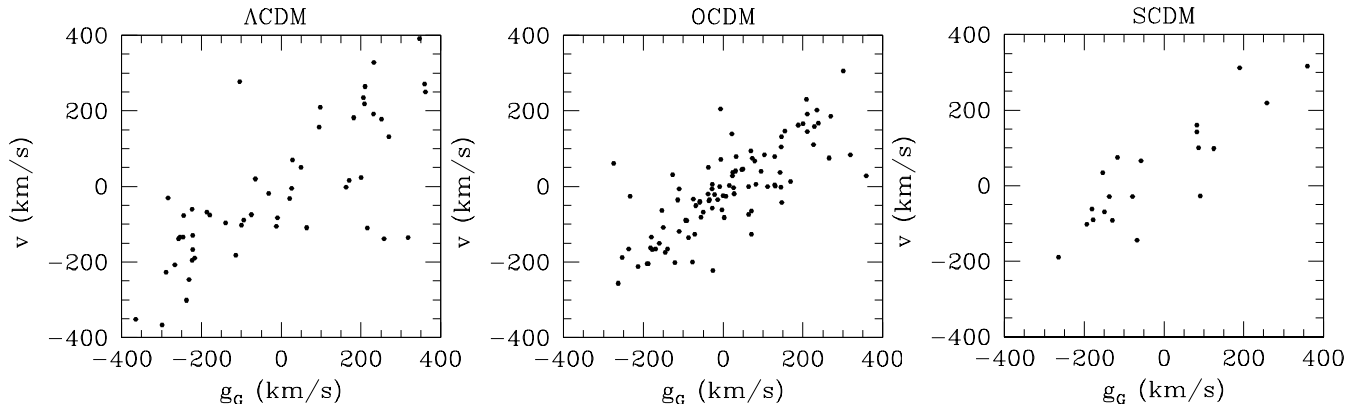


Figure 8. Peculiar velocity *vs.* global scaled acceleration of halos inside the LV for the same candidates as in Figure 4.

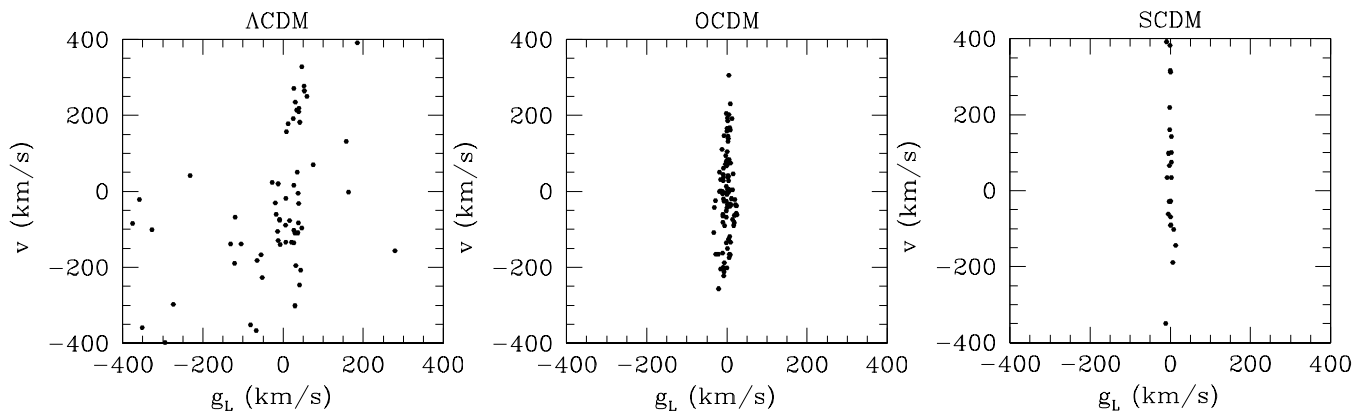


Figure 9. Peculiar velocity *vs.* local scaled acceleration for halos within the LV for the same candidates as in Figure 4.

6 DISCUSSION

We have clearly demonstrated in this paper that the W05’s analysis is not expected to yield a simple and clear correlation between the gravitational field calculated from the mass distribution within the local volume and the peculiar velocities of halos within that volume. This result invalidates W05’s basic assumption that the peculiar velocity field traces the gravitational field in a simple fashion, and therefore the statements concerning the role of the gravitational instability in the LV are not valid.

Setting aside issues concerning the practical limitations posed by observations of the LV and the uncertainty in estimating the dynamical mass of luminous galaxies there are three main theoretical reasons why W05’s analysis fails. The most obvious one is that the gravitational field is assumed to be traced by the galaxies, treated as point-like particles. Figs. 4 and 5 show the poor correlation between the actual gravitational field and the local field induced by the galaxies. Now, this poor correlation is mostly due to the sampling of the field by the galaxies, as manifested by Fig. 6 which shows a clear correlation between the global field and the local field that is induced by all dark matter particles in the LV.

The other reasons for the breakdown of the simple gravity - velocity relation of the linear theory are both related to the tidal field, hence the shear of the velocity field. The simpler reason is that in solving the Poisson equation one should

not neglect the homogenous solution, namely the tidal field. Now, in principle this can be easily corrected by adding a (spatial) linear term to the gravitational field that scales with the traceless shear tensor (Eq. 6 and Figure 12). Thus by adding six free parameters to the fitting procedure one might be able to account for the tidal field. However, the size of the LV is such that the spatial linear expansion of the tidal field would fail and lead to an incorrect estimation of the gravitational field. For the LV centered on the LG, the tidal effect of the LSC cannot be represented by a linear term.

The other reason for the inadequacy of the linear theory is more subtle. It has been shown that in the quasi-linear regime the growth of the density contrast depends on the magnitude of the shear tensor (Hoffman 1986, 1989; Zaroubi & Hoffman 1993; van de Weygaert & Babul 1994; Bertschinger & Jain 1994). The shear dependence introduces a non-local term in the equations that govern the growth of structure in the quasi-linear regime. Indeed, Fig. 8 shows a tight linear relation between the peculiar velocities and the scaled global gravitation field. Yet, the constant of proportionality is less than unity for all the LG-like objects in all the simulation (except of one single object) as is predicted by the linear theory prediction (in agreement with Hoffman (1989)). This behavior implies that under the optimal conditions of a full knowledge of the gravitational field a linear relation between the gravity and velocity field is expected within the LV around LG-like objects. However,

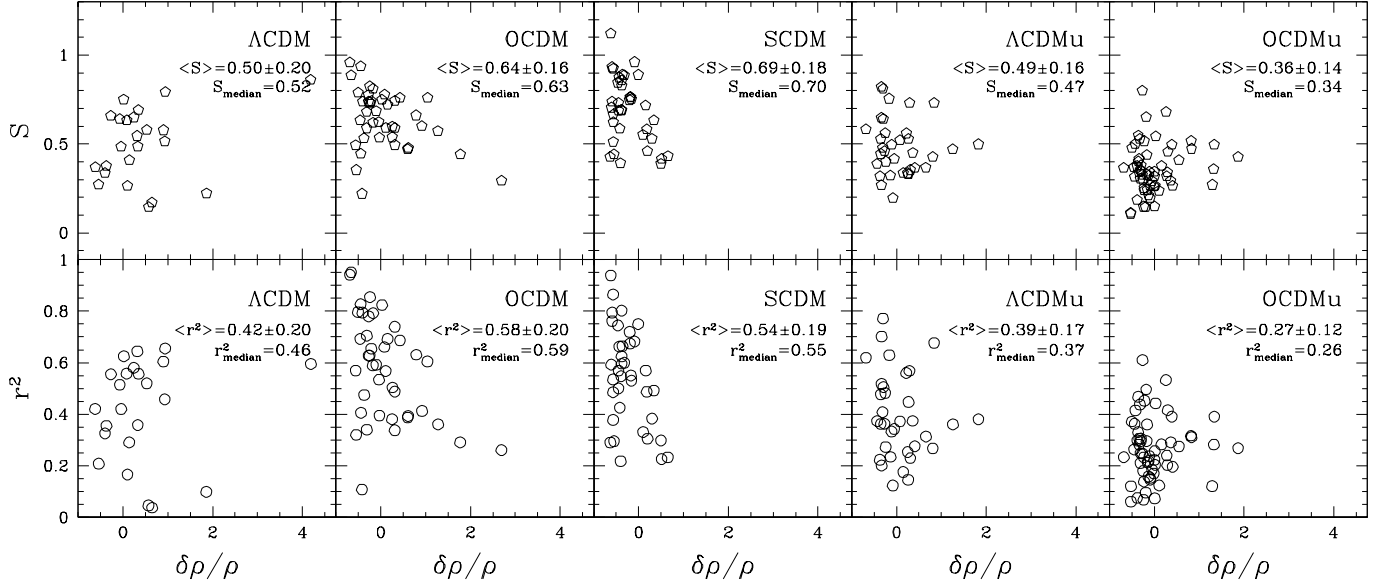


Figure 10. Same as Figure 5 but for the peculiar velocity *vs.* global scaled acceleration fits.

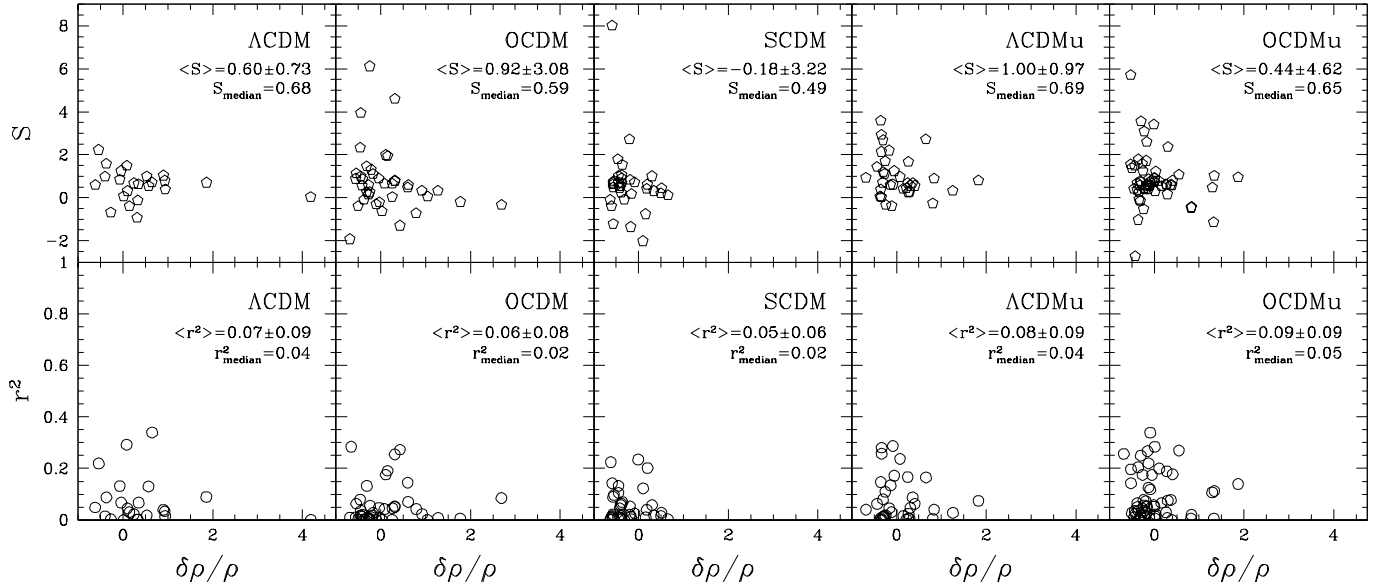


Figure 11. The same as Figure 5 but for the peculiar velocity *vs.* local scaled acceleration fit.

using the slope of the relation as a way of measuring Ω_m would underestimate its true value.

W05 attempted to find a simple linear relation between the peculiar velocities and local gravitational field of galaxies in the LV. A careful analysis of the dynamics within the LV around LG-like objects identified in constrained simulations of the local universe and in unconstrained simulations in flat- Λ CDM, OCDM and flat-matter only CDM cosmologies shows that a lack of correlation is to be expected. Hence we cannot support the claim that *'either dark matter is not distributed in the same way as luminous matter in this region, or peculiar velocities are not due to fluctuations in mass.'*

7 ACKNOWLEDGEMENTS

We appreciate very much the comments and discussions with Yago Ascasibar, Anatoly Klypin, Andrey Kravtsov, Stefan Gottlöber and Yaniv Dover. We would like to thank Astrophysikalisches Institut Potsdam for allowing us to use the Sansoucci supercomputer opteron clusters and to host us several times during the course of this work. We also thank CIEMAT (Spain) to allow us to use their SGI-ALTIX supercomputer and to NIC Jülich (Germany) for the access to the IBM-Regatta p690+ JUMP supercomputer. GY would like to thank also MCyT for financial support under project numbers AYA2003-07468 and BFM2003-01266. LAMV acknowledges financial support from MCyT (Spain) under project BFM2003-01266 and from Comunidad de Madrid through a PhD fellowship. YH acknowledges the support of

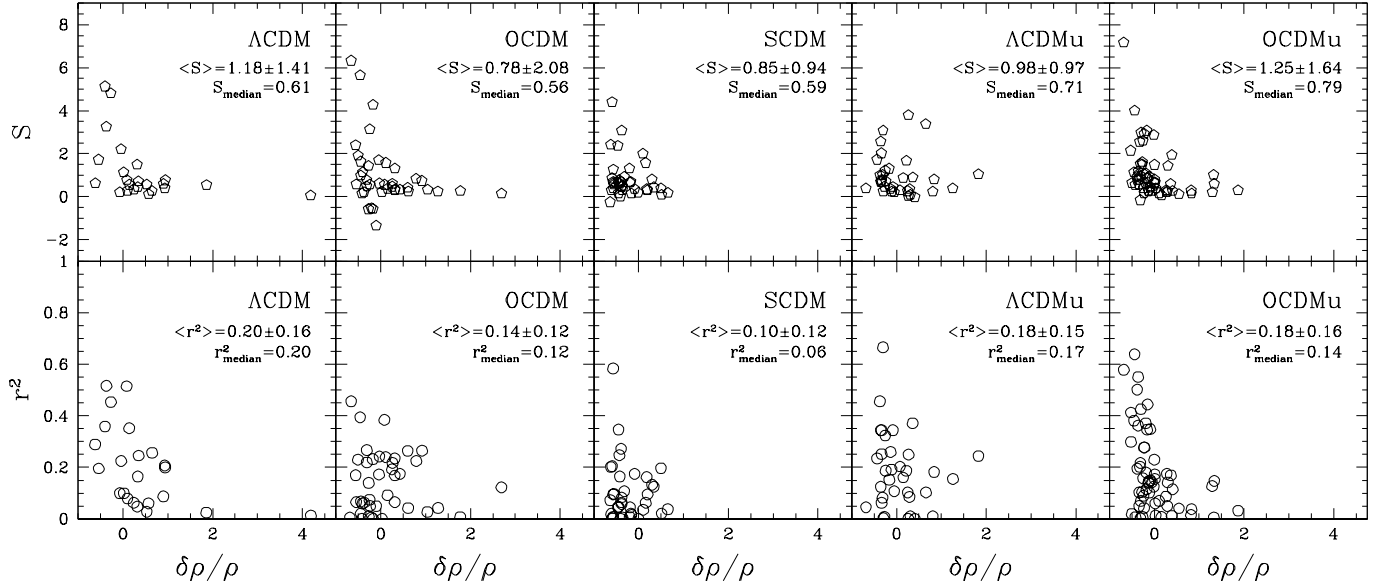


Figure 12. Same as Figure 11, but including the linear tidal field into the fitting procedure (see Eq. 6)

ISF-143/02, the Sheinborn Foundation and the DFG for a Mercator Gastprofessur at Potsdam University.

8 APPENDIX: THE GADGET ESTIMATION OF GRAVITATIONAL ACCELERATIONS

Throughout the paper the global and local gravitational accelerations have been compared. The local accelerations within the LV were calculated by summing the Newtonian pairwise field. This can be repeated for the global field by summing over all the particles of the simulation. This direct sum is computationally very costly and does not take into account the contribution of the infinite periodic boxes. We used instead the particle accelerations calculated by the TREE-PM algorithm by the GADGET code. The relation between the GADGET acceleration with \mathbf{g}_G is as follows:

The physical \mathbf{r} and comoving \mathbf{x} coordinates are related by: $\mathbf{r} = a\mathbf{x}$. The global gravitational field equals the physical acceleration of an object $\ddot{\mathbf{r}} = \mathbf{g}$.

Now, the GADGET code provides an acceleration-like term defined as:

$$\mathbf{f}_p = \frac{1}{a} \frac{d}{dt} (a \cdot \mathbf{v}_p) = \dot{\mathbf{v}}_p + H \cdot \mathbf{v}_p, \quad (7)$$

where \mathbf{v}_p is the peculiar velocity and a is the expansion scale factor.

It follows that

$$\ddot{\mathbf{r}} = \mathbf{f}_p + \mathbf{r} \frac{\ddot{a}}{a}. \quad (8)$$

Recalling that $\frac{\ddot{a}}{a} = -\frac{4\pi G \rho_c \Omega_0}{3}$ one gets at the end

$$\mathbf{g}_G = \mathbf{f}_p - \frac{1}{2} H^2 \Omega_0 \cdot \mathbf{r}. \quad (9)$$

This is the value we used for the global acceleration of each dark matter particle. The total acceleration of halos was computed by averaging this quantity over the entire number of particles belonging to each halo.

REFERENCES

- Bertschinger E., Jain B., 1994, *ApJ*, 431, 486
 Dolag K., Hansen F. K., Roncarelli M., Moscardini L., 2005, *MNRAS*, 363, 29
 Gill S. P. D., Knebe A., Gibson B. K., 2004, *MNRAS*, 351, 399
 Governato F., Moore B., Cen R., Stadel J., Lake G., Quinn T., 1997, *New Astronomy*, 2, 91
 Hoffman Y., 1986, *ApJ*, 308, 493
 Hoffman Y., 1989, *ApJ*, 340, 69
 Hoffman Y., Romano-Díaz E., Faltenbacher A., Jones D., Heller C., Shlosman I., 2006, in Mamon G. A., Combes F., Defayet C., Fort B., eds, *EAS Publications Series Constrained Simulations of Dark Matter Halos*. pp 15–18
 Karachentsev I. D., 2005, *AJ*, 129, 178
 Klypin A., Gottlöber S., Kravtsov A. V., Khokhlov A. M., 1999, *ApJ*, 516, 530
 Klypin, A., Kravtsov, A. V., Bullock, J. S., Primack, J. R., 2001, *ApJ*, 554, 903
 Klypin A., Hoffman Y., Kravtsov A. V., Gottlöber S., 2003, *ApJ*, 596, 19
 Klypin A., Rhee G., Valenzuela O., Holtzman J., Moorthy B., 2004, in Prada F., Martinez Delgado D., Mahoney T. J., eds, *ASP Conf. Ser. 327: Satellites and Tidal Streams The Rotation Curves of Dwarf Galaxies: a Problem for Cold Dark Matter?*. pp 3–+
 Kravtsov A. V., Klypin A., Hoffman Y., 2002, *ApJ*, 571, 563
 Lahav O., Lilje P. B., Primack J. R., Rees M. J., 1991, *MNRAS*, 251, 128
 Macciò A. V., Governato F., Horellou C., 2005, *MNRAS*, 359, 941
 Mathis H., Lemson G., Springel V., Kauffmann G., White S. D. M., Eldar A., Dekel A., 2002, *MNRAS*, 333, 739
 Peebles P. J. E., 1980, *The large-scale structure of the universe*. Princeton, N.J., Princeton University Press, 1980. 435 p.
 Reiprich T. H., Böhringer H., 2002, *ApJ*, 567, 716

- Springel V., 2005, MNRAS, 364, 1105
Tonry J. L., Dressler A., Blakeslee J. P., Ajhar E. A.,
Fletcher A. B., Luppino G. A., Metzger M. R., Moore
C. B., 2001, ApJ, 546, 681
van de Weygaert R., Babul A., 1994, ApJ, 425, L59
Whiting A. B., 2005, ApJ, 622, 217
Willick J. A., Courteau S., Faber S. M., Burstein D., Dekel
A., Strauss M. A., 1997, ApJ, 109, 333
Zaroubi S., Hoffman Y., 1993, ApJ, 414, 20
Zaroubi S., Hoffman Y., Dekel A., 1999, ApJ, 520, 413